Cui and Fall *Int J Concr Struct Mater* (2020) 14:23
https://doi.org/10.1186/s40069-020-0398-0

International Journal of Concrete Structures and Materials

RESEARCH Open Access

Numerical Simulation of Consolidation Behavior of Large Hydrating Fill Mass

Liang Cui and Mamadou Fall*

Abstract

Underground mined-out voids need to be backfilled for the stability of the surrounding rock and also to increase ore extraction from adjacent pillars. One of the relatively newer means is cemented paste backfilling, which has been extensively adopted in underground mining operations around the world. During and after the placement of cemented paste backfill (CPB) into stopes, complex multiphysics (thermal, hydraulic, mechanical and chemical) processes take place in the large mass of CPB and could affect its consolidation behavior. An analysis of the consolidation process in CPB mass is essential for the assessment of CPB behavior and cost-effective designs in practice. In this paper, multiphysics simulation of the consolidation behavior of CPB mass is performed under different conditions, including the mixture recipe, and backfilling, drainage, surrounding rock and curing conditions. It is found that the in situ consolidation behavior of CPB structures is a function of the multiphysics processes that occur in the cementing backfill mass. Moreover, the rock mass conditions, including the geometry and rock wall roughness, influence the consolidation process of CPB structures. Cement content, curing time and backfilling rate play a crucial role in the consolidation process of CPB. The obtained results can facilitate a better understanding of the consolidation behaviour of CPB for backfill designers and engineers, and thus contribute to enhance the engineering of CPB structures.

Keywords: mine, cemented paste backfill, tailings, consolidation, soft concrete, THMC, multiphysics

1 Introduction

Cemented paste backfill (CPB) is an engineered mixture of tailings (man-made soils), hydraulic binder and water (Fall et al. 2007a, b). After preparation in a backfill plant usually located on the mine surface, the fresh CPB is transported into underground stopes (mined-out voids) via reticulated pipelines and/or gravity system (Haiqiang et al. 2016). As the hardening process of the large fill mass progresses, CPB provides ground support to the adjacent stopes (Ghirian and Fall 2014; Cui and Fall 2016a, b; Zhang et al. 2015), which can maximize ore recovery (Yilmaz et al. 2003; Benzaazoua et al. 2004; Fall et al. 2010), and reduce surface subsidence (Hassani et al. 2001a, b; Jehring and Bareither 2016). Moreover, the relatively high amount of binder and solid content ensure that the CPB mass gains strength more quickly compared to rockfill and hydraulic fill (Cui and Fall 2015a, b). In addition, the application of CPB enables a reduction of approximately 50–60% of the sulphidic tailings deposited on the surface (Khaldoun et al. 2016; Potvin and Thomas 2005). Hence, from an environmental point of view, cemented paste backfilling is an alternative means of reducing environmental issues (e.g., acid mine drainage) associated with surface tailings disposal. Consequently, cemented paste backfilling has been widely employed in the underground mines throughout the world (Haiqiang et al. 2016).

In engineering practices, mechanical stability is considered as one of the most important design criteria of CPB structures (Fall et al. 2015). The mechanical performance of CPB structures is closely related to the consolidation process in the CPB. The backfilling process is flexible (i.e., the process is continuous or carried out in different filling stages), which means that the dissipation of pore water pressure (PWP) will take place in CPB due to water drainage through the barricade (a retaining wall built to

*Correspondence: mfall@uottawa.ca
Department of Civil Engineering, University of Ottawa, 161 Colonel By, Ottawa, ON K1N 6N5, Canada
Journal information: ISSN 1976-0485 / eISSN 2234-1315

contain backfill material) and/or from the surrounding fractured rock mass, and/or water consumption caused by binder hydration, which can result in an increase in the effective stress and strength (Cui and Fall 2015a, c). Moreover, binder hydration induced chemical shrinkage will further contribute to volume changes (Cui and Fall 2015a) and thus to the densification of CPB, which is desirable for increased strength. In addition, the temperature dependence of binder hydration (Schindler and Folliard 2003) means that the heat transfer and resultant temperature changes must be taken into account in the analysis of CPB performance. Therefore, the consolidation process is controlled by complex multiphysics (i.e., thermo-hydro-mechanical-chemical, THMC) processes that occur in the CPB. Apart from the coupled THMC processes, the rock mass/backfill interaction (interface) can affect the stress distribution and thus the volume changes in the fill mass (Fahey et al. 2009). Specifically, with the development of consolidation, relative displacement along the rock mass/CPB interface will occur, and the resultant interface stress will reduce the influence of the self-weight stress of CPB (i.e., the arching effect will occur) (Fang and Fall 2018), which will result in non-uniform volume changes in the CPB. Therefore, analysis of backfill-rock interface behavior in stopes is essential for the assessment of the consolidation behavior of CPB mass.

However, conventional analysis techniques on consolidation, such as Terzaghi (1943) consolidation theory and Biot (1955) consolidation theory, only focus on the volume contraction behavior triggered by the dissipation of excess pore water in saturated soils or porous media (Ceccato and Simonini 2016; Ai and Hu 2015), namely, the analysis of coupled hydro-mechanical (HM) processes. Therefore, these classical theories are not suitable for the assessment of the coupled THMC consolidation behavior of CPB materials. To address this problem Cui and Fall (2016a), developed a fully coupled multiphysics model that analyzes the consolidation process in CPB and incorporates the THMC processes that occur in CPB and thus affect its consolidation behavior. This new approach fully considers the effect of self-weight, pore water flow and drainage, chemical shrinkage, thermal expansion, and temperature on the binder hydration. Moreover, Cui and Fall (2017) developed an elastoplastic model to analyze changes in the interface behavior during the interaction of rock mass/backfill. In the elastoplastic model, the hardening/softening behavior, chemical hardening process and the effect of the rock wall roughness on the interface properties (interface adhesion and friction angle) are taken into account. Therefore, the fully coupled multiphysics model for analyzing consolidation problems and the evolutive elastoplastic interface model will allow prediction of the consolidation behavior of CBP at the field scale. In the present study, these two models are integrated to numerically model the consolidation behavior of CPB mass under various field conditions, including the filling rate, stope geometry and inclination angle, rock wall roughness, mix components (cement content) and drainage conditions. The integration of these two models (multiphysics and elastoplastic interface models) is necessary in order to describe the consolidation behaviour of the CPB when arching effect takes place, i.e. in the case of narrow stopes. The arching effect significantly affects the distribution and magnitude of stress within the CPB, thus its consolidation behaviour.

2 Mathematical models

In this study, two models are integrated to examine the volume changes of the fill mass in a stope: a fully coupled multiphysics model that analyzes the consolidation process in CPB as proposed by Cui and Fall (2016a), and an evolutive elastoplastic model that analyzes changes in the interface behavior during the interaction of rock mass/backfill, as provided by Cui and Fall (2017). Details on these two models including the assumptions made, model derivation and determination of model coefficients are provided in Cui and Fall (2016a, 2017). A brief description of the two models is provided in Sects. 2.1 and 2.2, respectively.

2.1 Fully coupled multiphysics model for consolidation process

Due to the strongly coupled THMC processes that occur in fill mass, the consolidation behavior of CPB in a slurry state is a very complex process compared to that of conventional geomaterials, such as natural soils. A multiphysics model for the consolidation behavior of CPB must satisfy the principle of pore space continuity (Cui and Fall 2016a), which requires that the pore space changes associated with the CPB skeleton and solid phase must be consistent with the volume changes in the pore water and pore air. Hence, based on the principle of pore space continuity, a consolidation equation based on multiphysics can be derived as follows and is elaborated in detail in Cui and Fall (2015a, 2016a):

$$\left\{[SP_w + (1-S)P_a]\frac{1-2\upsilon}{E}\frac{\partial \alpha_{Biot}}{\partial \xi} - \left\{\frac{\sigma + \alpha_{Biot}[SP_w + (1-S)P_a]}{E}\right\}\left\{\frac{9[1-2\upsilon]}{E}\frac{\partial E}{\partial \xi} + 18\frac{\partial \upsilon}{\partial \xi}\right\}\right.$$
$$\left. -\alpha_{Biot}(P_a - P_w)\frac{1-2\upsilon}{E}\left\{[1 - S_e(P_w, P_a, \xi)]\frac{\partial \theta_r}{\partial \xi} + (n-\theta_r)\frac{\partial S_e}{\partial \xi}\right\} - \frac{(v_{ch-w} + v_{ab-w})R_{n-w/hc}/(1-n)}{(w/c)v_w + v_c + (1/C_m - 1)v_{tailings}}\right\}\frac{\partial \xi}{\partial t}$$
$$+ \frac{1-2\upsilon}{E}\frac{\partial \sigma}{\partial t} + \alpha_{Biot}\frac{1-2\upsilon}{E}\left\{S - (P_a - P_w)(n-\theta_r)\frac{\partial S_e}{\partial P_w}\right\}\frac{\partial P_w}{\partial t} + \frac{\partial \lambda_p}{\partial t}\frac{\partial Q_{CTB}}{\partial I_1} + \alpha_{Ts}\frac{\partial T}{\partial t} \tag{1}$$
$$+ \alpha_{Biot}\frac{1-2\upsilon}{E}\left\{(1-S) - (P_a - P_w)(n-\theta_r)\frac{\partial S_e}{\partial P_a}\right\}\frac{\partial P_a}{\partial t}$$
$$= -\left\{(1-n) + \alpha_{Biot}(P_a - P_w)\frac{1-2\upsilon}{n^2 E}[n(1-n)S_e + (1-S_e)\theta_r]\right\}\frac{\partial n}{\partial t}$$

where S is the degree of saturation; P_w and P_a denote the PWP and pore-air pressure, respectively; υ and E denote the Poisson's ratio and elastic modulus, respectively; α_{Biot} is the Biot's coefficient; ξ is the degree of binder hydration; σ is a total stress tensor; S_e is the effective degree of saturation; θ_r is the residual water content; n refers to the CPB porosity; v_w, v_{ch-w}, v_{ab-w}, $v_{tailings}$ and v_c denote the specific volume of the capillary water, chemically consumed water, physically adsorbed water, tailings and cement respectively; $R_{n-w/hc}$ means the mass ratio of the chemically consumed water and hydrated cement; w/c is the water to cement ratio; C_m is the binder content; t refers to the elapsed time; λ_p denotes a non-negative plastic multiplier; Q_{CTB} is a plastic potential function; I_1 represents the first stress invariant; and α_{Ts} refers to a coefficient of the thermal expansion of the solid phase in the CPB. The determination of the model parameters mentioned above is given in Cui and Fall (2015a, 2016a).

As demonstrated in the consolidation model (i.e., Eq. (1)), the chemical process is incorporated into the volume changes in CPB through the variable ξ, namely, the degree of binder hydration. To characterize the progress of the hydration reaction in CPB, the following exponential equation proposed by Schindler and Folliard (2003) is adopted:

$$\xi(t) = \left(\frac{1.031 \cdot w/c}{0.194 + w/c} + 0.5 \cdot X_{FA} + 0.30 \cdot X_{slag}\right) \cdot \exp\left\{-\left\{\tau \Big/ \int_0^t \exp\left[\frac{E_a}{R}\left(\frac{1}{T_r} - \frac{1}{T}\right)\right]dt\right\}^{\beta}\right\} \tag{2}$$

with

$$E_a(T) = \begin{cases} 33{,}500 + 1{,}470 \times (293.15 - T) & T < 293.15K \\ 33{,}500 & T \geq 293.15K \end{cases}$$

where τ and β respectively represent the time parameter (hours), and hydration shape parameter, T_r refers to the reference temperature (K), R is the ideal gas constant (8.314 J/mol/K), E_a refers to the apparent activation energy (J/mol), and X_{slag} and X_{FA} denote the weight proportion of the blast furnace slag and fly ash relative to the total binder mass, respectively. In accordance with the definition of the degree of binder hydration (i.e., Eq. (2)), the influence of temperature, mixture recipe and elapsed time are incorporated to determine the progression of the hydration reaction.

2.2 Evolutive elastoplastic interface model

To incorporate the effect of the interface behavior between the CPB/rock mass into the analysis of the consolidation process, an evolutive elastoplastic interface model developed by Cui and Fall (2017) is adopted to assess the interface shear stress in the present study. In this model, the changes of the yield surface in the stress space is characterized by a modified Drucker-Prager (D-P) yield function F_{intf}, and the changes in the direction of the plastic displacement is determined with a non-associative plastic flow rule (i.e., the plastic potential function Q_{intf} differs from the yield function F_{intf}).

$$F_{intf}(I_1, \sqrt{J_2}, \xi, \Delta_\kappa) = \sqrt{J_2} + \alpha_{intf}(\xi, \Delta_\kappa)\left[I_1 - C_{intf}(\xi)\right] = 0 \tag{3}$$

$$Q_{intf} = \sqrt{J_2} + 2\sqrt{3}\sin(\psi_{intf})I_1 \Big/ \left[9 + 3\sin(\psi_{intf})\right] \tag{4}$$

where J_2 is a second deviatoric stress invariant, Δ_κ is the effective plastic displacement, α_{intf} and C_{intf} are the yield function parameters, and ψ_{intf} denotes the interface dilation angle which will change with binder hydration and normal stress level acting on the interface. Details on how the interface model coefficients are determined can be found in Cui and Fall 2017).

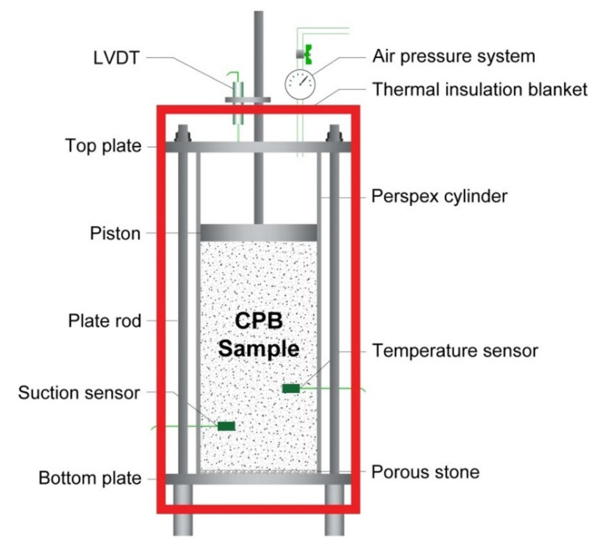

Fig. 1 Schematic diagram of THMC pressure cell

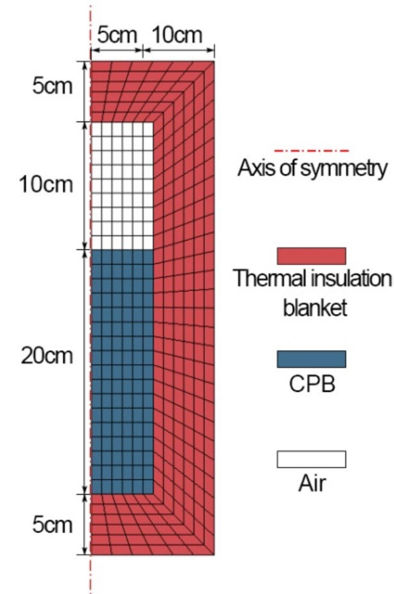

Fig. 2 Geometry and mesh of simulated model of cell test

3 Model Validation

The two models presented above are first implemented into COMSOL Multiphysics (a commercial finite element method (FEM) code software; Comsol 2015). Then, the integrated model is validated against results obtained from laboratory investigations on the consolidation behavior of CPB and field measurements. Typical examples and results that validate the model are then presented below. Additional examples and results that validate the model are also presented elsewhere (Cui and Fall 2015a, b, c, 2016a, 2017).

3.1 THMC Consolidation Test—Lab

To study the consolidation behavior of CPB, a series of pressure cell tests were conducted by using a THMC pressure cell apparatus (see Fig. 1). This pressure cell apparatus was originally developed by Ghirian and Fall (2013), which is mainly composed of an air pressure system, a Perspex cylinder [10 cm (diameter) × 30 cm (height)], an air-pressure driven piston and two plates with three tie rods to hold the THMC cell. The adopted air pressure system can apply up to 600 kPa of air pressure onto the CPB sample to simulate the increase of self-weight stress in a stope during backfilling operations. To collect the data, a linear variable displacement transformer (LVDT) was mounted onto the top of the cell to record the vertical settlement, and a suction meter (model: MPS-2) and a temperature sensor (model: 5TE) were installed inside the THMC cell. Artificial silica tailings (medium size tailings; contain 45% of particles with size ≤ 20 μm), Portland cement Type 1 (4.5 wt%) and tap water (w/c = 7.6) were used to prepare the CPB samples. After placement, the pressure cell was covered with a thermal insulation blanket to slow down the heat transfer between the CPB sample and the surrounding environment. In terms of the application of air pressure, the applied pressure was gradually increased to 150 kPa in the first 12 h. Then, the pressure was increased every 24 h until 600 kPa (an average filling rate equal to 0.131 m/h was used in this study). Moreover, two different initial

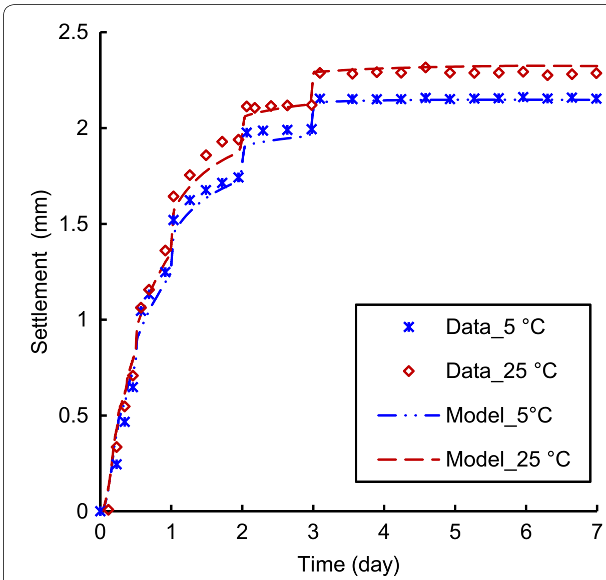

Fig. 3 Comparison of predicted results and experimental data for settlement

temperatures of the CPB (5 °C and 25 °C) were used to investigate their effects on the consolidation process.

A 2D axisymmetric model was used to simulate the pressure cell test. The geometry model and mesh are presented in Fig. 2.

A comparison of the simulation results and monitored data from the vertical settlement is plotted in Fig. 3. It can be clearly seen that the simulated results are in good agreement with the recorded data in terms of both changes in trend and magnitude. Moreover, the results show that (1) the vertical displacement increases with applied air pressure, which confirms that the developed model is able to capture the effect of backfilling operations on the self-weight stress, and thus its effects on the consolidation behavior of CPB; (2) the initial temperature of the CPB has a significant effect on its vertical settlement. As shown in Fig. 3, the vertical settlement of the CPB with an initial temperature of 25 °C (can represent the initial temperature of CPB in summer season) increases by approximately 8% compared to that of the CPB with an initial temperature of 5 °C (can represent the initial temperature of CPB in a cold mining region) at 7 days; (3) during each curing age, the air pressure applied is constant but the vertical settlement continues to increase, which indicates that chemical shrinkage contributes to the volume changes in the CPB.

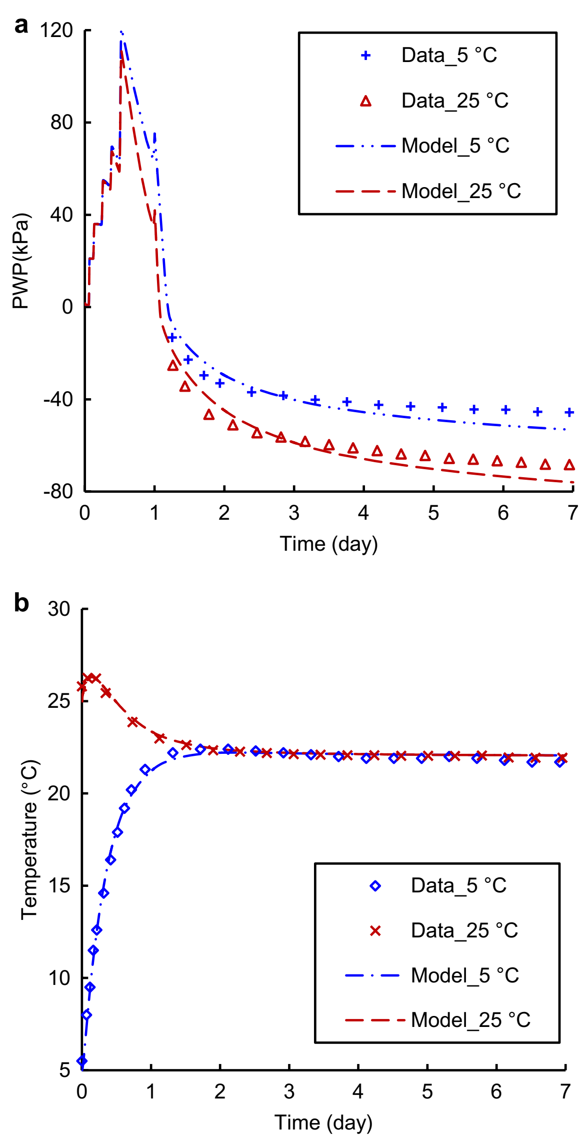

Fig. 4 Comparison of predicted results and measured data: **a** PWP; **b** temperature

Apart from the settlement, the changes in the PWP (Fig. 4a), and temperature (Fig. 4b) can also be accurately captured by using the developed model. From these two figures, it is evident that (1) the major changes in the PWP and temperature occur at the very early ages, which coincides with changes in the vertical settlement (see Fig. 3). This is because the binder hydration takes place rapidly at the very early ages. As a result, a relatively large volume of pore water is consumed, which in turn results in a significant change in the PWP. Meanwhile, the rapid binder hydration releases a large amount of heat and thus affects the temperature in the CPB at the early ages; (2) similar to the obtained results from the vertical settlement, the initial temperature of the CPB can also impose a significant impact on the changes in the PWP and temperature. The good agreement between the numerical simulations and results from the laboratory tests further confirms that the developed model can reliably simulate the consolidation behavior of CPB.

3.2 Field Study 1-Undrained CPB Mass

To study the field behaviors of CPB, a series of field monitoring programs have been carried out (e.g., Thompson et al. 2009; Helinski et al. 2010; Li et al. 2014). Although the reported field data are limited to total stress (e.g., Hassani et al. 2001a, b), PWP (e.g., Shahsavari and Grabinsky 2015) and temperature (e.g., Williams et al. 2001) in the CPB, the obtained results can still provide useful information on the field behaviors of CPB, including the consolidation process.

In the present study, the predicted results are compared with the measured data from a field monitoring program conducted by Belem et al. (2004) at the Doyon Gold (DG) Mine (Canada). The investigated stope has a height of 29 m and a width of 11 m with a dip of 90° and an azimuth of 90°. A backfilling operation that consists of two stages was adopted, which includes a plug layer

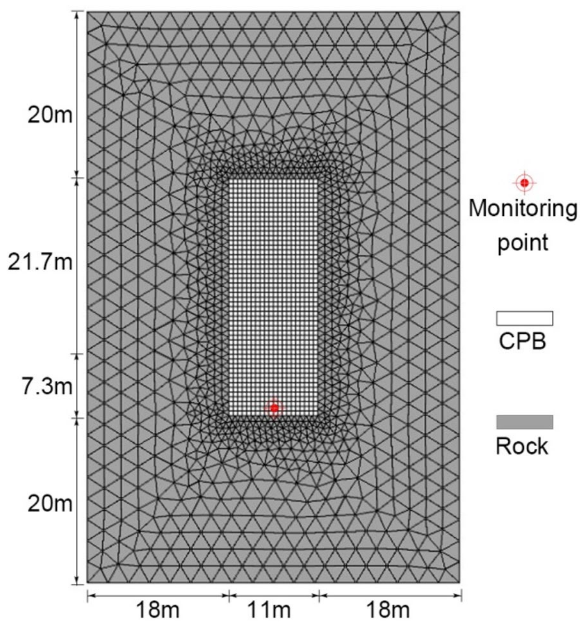

Fig. 5 Mesh and geometry of simulated stope at DG Mine

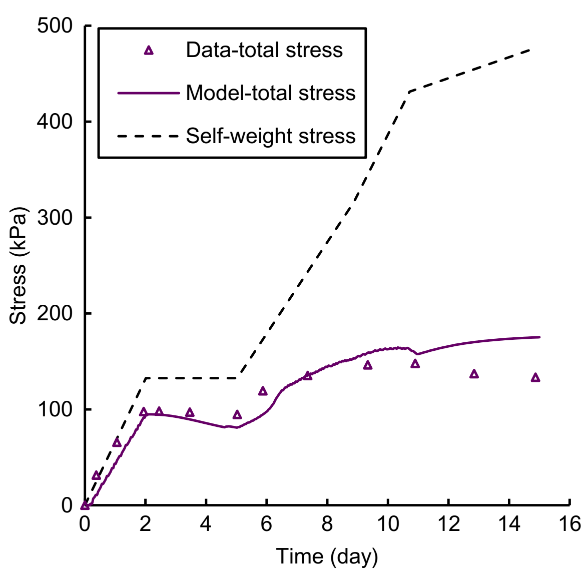

Fig. 6 Comparison of predicted results and measured total stress values at DG Mine

(cement content: 7% and solid content: 70%). After 3-days of curing, the residual stope was filled with CPB with a cement content of 3% and a solid content of 70%. An earth pressure cell (TPC series) was used to record the changes in the total pressure at the stope base (elevated 0.6 m). Water drainage was not allowed on this stope. The corresponding mesh and stope geometry are shown in Fig. 5.

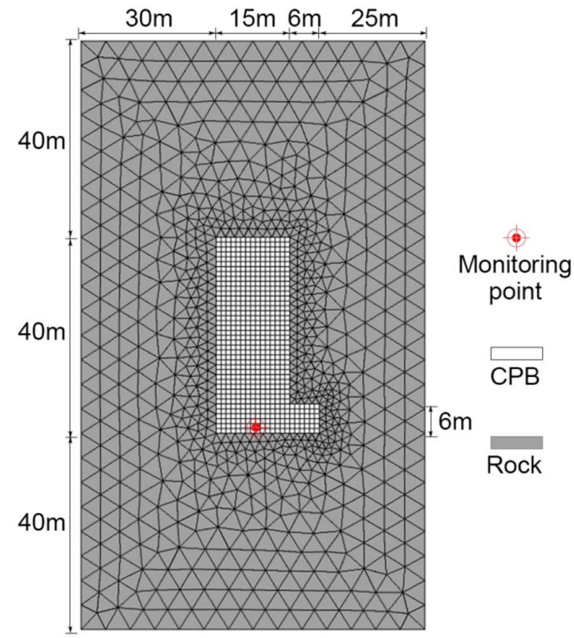

Fig. 7 Mesh and geometry of simulated stope at Kanowna Belle mine

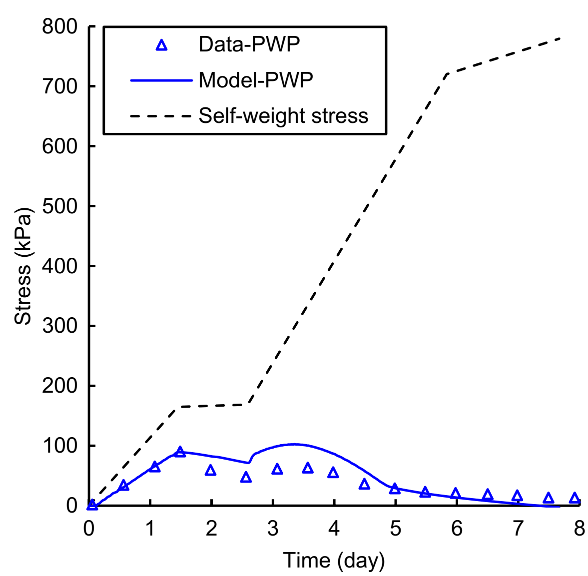

Fig. 8 Comparison of predicted results and measured values of PWP at Kanowna Belle mine

A comparison of the predicted results and monitored total stress values is presented in Fig. 6. Based on the obtained results, it can be found that (1) as expected, the filling processes have significant impacts on the changes in total stress, especially during the plug placement stage; (2) during the curing of the plug layer (from the 2nd to the 5th day), there is a slight reduction in total stress which gradually took place and can be attributed to the transfer of stress from the fill mass to the rock walls (arching effect) with the development of consolidation of the CPB mass; and (3) after the residual filling commenced (from the 5th day), the total stress shows a relatively limited increase compared with that observed during the plug-fill, which further contributes to the discrepancy between the total stress and self-weight stress. From Fig. 6, it can be seen that the predicted results are in good agreement with the monitored data. Hence, the developed model is able to reliably assess the changes in total stress in CPB under undrained conditions.

3.3 Field Study 2-Drained CPB Mass

To investigate the field behavior of CPB under drained conditions, in situ measurements were conducted by Helinski et al. (2010) in the Kanowna Belle mine. In this monitoring program, a piezometer was installed at the center of the stope base to monitor the changes in the PWP in the CPB. The backfilling strategy was to carry out filling in two stages. Pore-water drainage through the retaining structure (i.e., the barricade) was allowed. More details on the CPB design are provided in Helinski et al. (2010). The geometry model and mesh are presented in Fig. 7.

As can be seen in Fig. 8, the changes in the PWP are captured well by the developed model. Specifically, during the first stage of filling, the PWP gradually increases with filling. After 1.4 days (the commencement of the curing of the plug layer), dissipation of the PWP is observed in the CPB, which is attributed to the water drainage through the barricade and binder hydration induced water consumption (i.e., the self-desiccation process). The dissipation of the PWP can directly contribute to reductions in pore space and thus to the consolidation process of CPB. In addition, from Fig. 8, it can be observed that the effect of the residual filling on PWP is minimal, and a slight

Table 1 Input parameters, and initial and boundary conditions

Input item	Parameter	Value
CPB	Stope geometry (m)	15 m (W) × 30 m (H)
	Inclination angle (°)	90
	Cement content (wt%)	Residual fill: 4.5 (60.4 kg/m^3), and plug fill: 7 (80.2 kg/m^3)
	w/c ratio	7.6
	Initial void ratio	1
	Backfilling rate (m/h)	0.5
	Backfilling strategy	2-stages of filling with 1-day plug
Rock mass	Density (kg/m^3)	2500
	Young's modulus (GPa)	30
	Poisson's ratio	0.3
	Thermal conductivity (W/m K)	3.9
	Heat capacity (J/kg K)	790
Mechanical module	Top surface	Free
	Lateral sides	Roller
	Bottom side	Fixed
	Volume force	Gravity
Hydraulic module	Top surface	No flow
	Lateral sides	No flow
	Bottom side	No flow
	Volume force	Gravity
	Initial value	Hydraulic head = 0
Thermal module	Top side (°C)	25
	Lateral sides (°C)	25
	Bottom side (°C)	25
	Initial temp. (°C)	25

wt% weight percentage with respect to the total weight of the solid phase in CPB

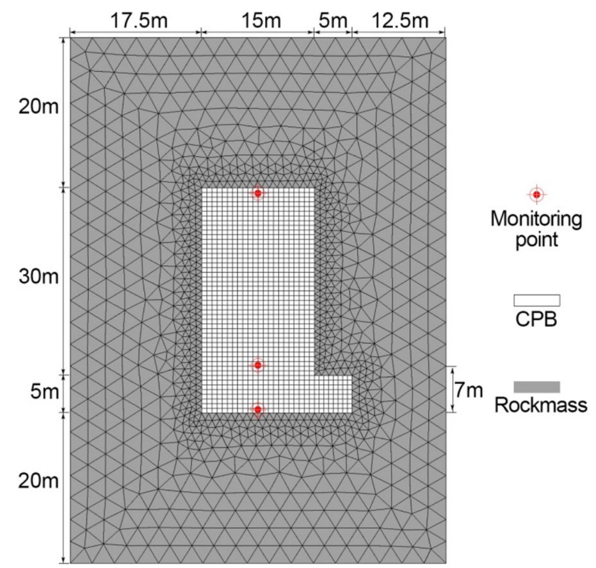

Fig. 9 Mesh and geometry of control CPB and stope

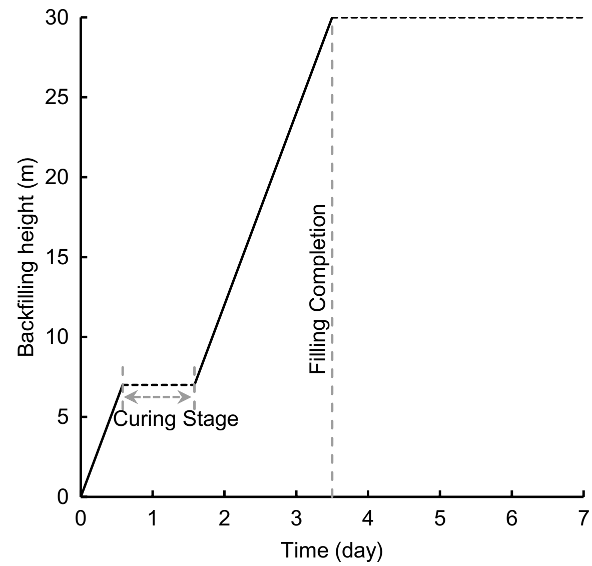

Fig. 10 Backfilling operation for the control stope

increase in the PWP appears during the middle of the second and third days. Then, the PWP decreases regardless of the backfilling that followed, which can further contribute to the volume changes in the fill mass. Therefore, the good agreement between the predicted results and field data further validates the predictive ability of the developed model for CPB behavior under drained conditions.

4 Model Applications

After the successful validation of the models, a series of numerical simulations were carried out to investigate the field consolidation behavior of CPB mass under various conditions or with various factors. They included different curing ages, stope geometries, inclination angles, rock wall roughness, cement contents, backfilling rates and strategies, and drainage conditions. To assess the consolidation behavior of CPB under different conditions, a control stope with a predefined geometry, backfilling strategy and rate, mix recipe and curing condition was utilized as a reference. All numerical investigations were performed by modifying the conditions of the control stope. Details on the input parameters, and initial and boundary conditions of the control stope are listed in Table 1.

The geometry and mesh for the control CPB mass and stope are presented in Fig. 9. Three monitored points are examined: 29.5 m, 7 m and 0.5 m from the stope floor. These three monitored points are used to investigate the development of consolidation with curing time. Moreover, the monitored point of 7 m is located on the interface where the filling takes place, and thus can provide useful information about the backfilling operation including both the curing time of the plug layer and the effects of subsequent filling. Therefore, this monitored point is used to study the effects of the stope geometry, rock wall roughness, mix components, and backfilling and drainage conditions.

The backfilling strategy (filling operation carried out in two-stages) and rate (0.5 m/h) adopted in the control stope is presented in Fig. 10. After the first layer of CPB was placed into the stope, the fresh plug layer was

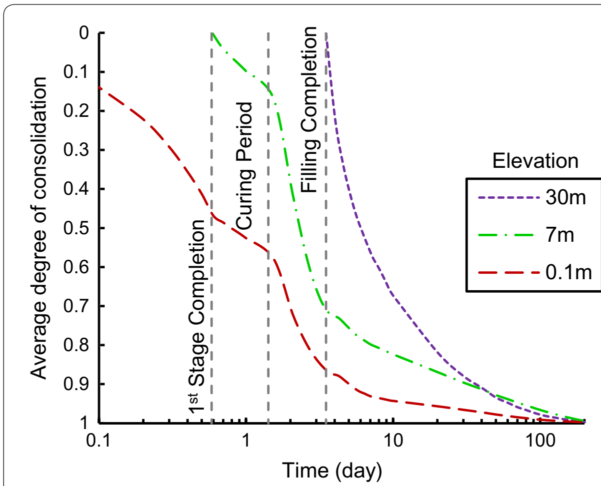

Fig. 11 Variation of average degree of consolidation with curing time

allowed to cure for 1 day. Then, residual backfilling was carried out.

During and after filling, water drainage through the barricade was allowed. For the numerical implementation of the drained condition in the CPB, a water mass flux boundary condition was incorporated into the hydraulic module and applied on the right vertical side of the drawpoint. The water mass flux can be computed by multiplying the pore water density and its velocity through the retaining wall. The latter can be determined by using Darcy's law.

4.1 Effect of Curing Time

With curing time, binder hydration induced chemical shrinkage, water drainage through the barricade and/or fractured rock mass, and self-weight induced volume changes will contribute to the consolidation process in CPB. Moreover, due to the temperature dependence of binder hydration (Cui and Fall 2015a; Schindler and Folliard 2003), the heat generated by hydration reactions, and heat transfer between the CPB and surrounding rock can affect the chemical reaction rate and thus the consolidation process. Therefore, the effect of curing time on the consolidation behavior of CPB needs to be examined. Figure 11 presents the changes in the average degree of consolidation (i.e., the ratio of the vertical settlement at any time and the final settlement) for three different heights of the CPB. From this figure, the following characteristics that depict the changes in the consolidation process in the CPB are found:

i. CPB strongly demonstrates time-dependent consolidation behavior. The changes in the rate of consolidation with time (i.e., the slope of the consolidation curve) can be attributed to the hardening process of the CPB skeleton, reduction in the rate of hydration with time, and reduction in the permeability of the CPB. Specifically, in terms of the effect of the hardening process, the CPB stiffness will be progressively increased by enhancing the bonding between tailings particles with the precipitation of binder hydration products in the capillary pore space [35, 36], and the densification process through the consolidation of the CPB (Tariq, 2012; Fall et al. 2007a, b). The resultant stiffer CPB can resist larger loadings and thus reduce the rate of consolidation under a constant filling rate with time. Secondly, in terms of the effect of the rate of binder hydration, previous experimental studies (e.g., Ghirian and Fall 2015; Han et al. 2016) on cementitious materials have found that precipitated hydration products on the surface of an unhydrated binder can delay water diffusion into the unhydrated binder particles. As a result, there will be gradual reductions in the rate of binder hydration, and thus the contribution of chemical shrinkage to the development of consolidation is gradually reduced. In addition, another contributor to the delay in consolidation is the reduction of CPB permeability as consolidation of the CPB proceeds (Helinski et al. 2010) and thus gradually reduces the amount of water drainage through the barricade, which can in turn delay seepage-induced consolidation. Consequently, the time rate of the change in consolidation shows a decreasing trend with time.

ii. Moreover, CPB also shows a distinct consolidation behavior between the filling stages and cur-

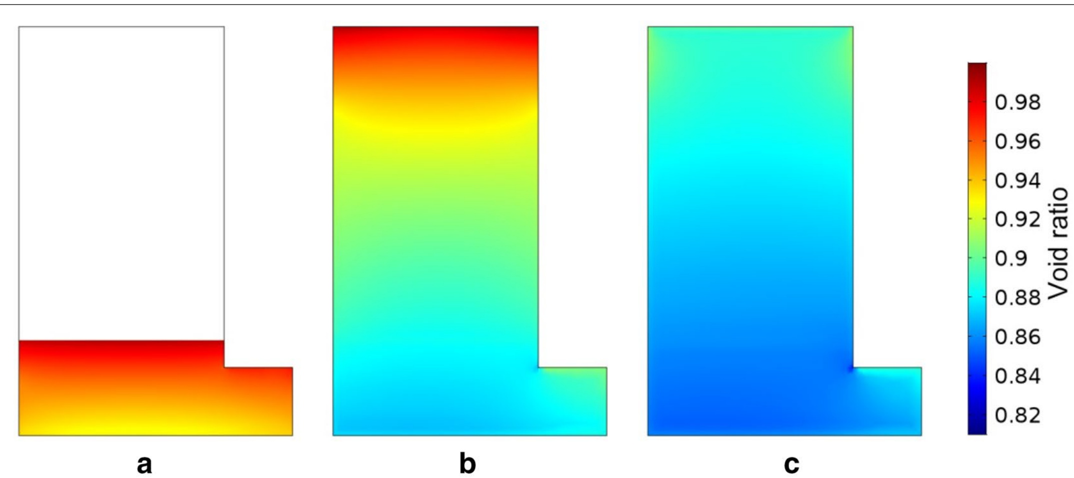

Fig. 12 Changes in void ratio with curing time: **a** 14 h (completion of plug filling); **b** 84 h (completion of filling operation); and **c** 168 h

ing of the plug layer (i.e., 1-day of curing from 14 h to 38 h). Specifically, greater volume changes take place during the filling stages due to the increase in the overburden stress by the placement of fresh CPB. With increased self-weight stress, the CPB becomes more consolidated.

iii. In addition, by comparing the consolidation behavior at three different heights of the CPB mass, it can be observed that the CPB becomes more consolidated at greater heights for any given filling and curing time. This is because the relatively fresh CPB is poured at higher elevation in backfilling operations that take place in different stages. The fresh CPB has relatively low stiffness, higher permeability and faster rate of hydration. Hence, CPB becomes more consolidated with greater height. Consequently, the development of spatially non-uniform consolidation appears in the CPB.

To further illustrate the spatial distribution and development of the consolidation process in CPB, void ratio changes in the control stope are investigated and presented in Fig. 12. It can be observed that the development of consolidation of CPB is relatively uniform at a given height at the early ages (see Figs. 12a, b). With time, the non-uniform distribution of the void ratio becomes apparent, especially in the vicinity of the rock walls (see Fig. 12c). The non-uniform change in the void ratio is mainly attributed to the arching effect (Yilmaz et al. 2018). In addition, Fig. 12 shows that a major change in the void ratio takes place around the layer interface when the filling takes place in stages (i.e., 7 m from the stope base). This is due to (1) the distinct interface properties and inconsistent rate of consolidation near the layer interface (Cui and Fall 2016a), and (2) the difference in the refinement of the capillary pore space around the layer interface when filling takes place in stages. More specifically, the interface adhesion and friction angle will be gradually increased during the 1-day of curing. Therefore, the first layer (i.e., the plug layer) is able to form higher shearing resistance along the backfill/rock-wall interface compared to the second CPB layer. Moreover, the precipitation of hydration products also plays an important role in the reduction of the void ratio. Compared with the fresh residual CPB layer, more hydration products can form in the pore space of the plug layer, which can contribute to the changes in the void ratio near the layer interface. In addition, compared to the plug layer, binder hydration occurs more quickly in relatively fresh CPB (i.e., second layer), which causes significant chemical shrinkage and thus contributes more to the development of consolidation of the CPB along the layer interface. Consequently, the variations in the void ratio near the interface of the different backfill layers gradually become more pronounced with time. Similar results have been found in previous studies on CPB (e.g., El Mkadmi et al. 2013; Li and Aubertin 2009).

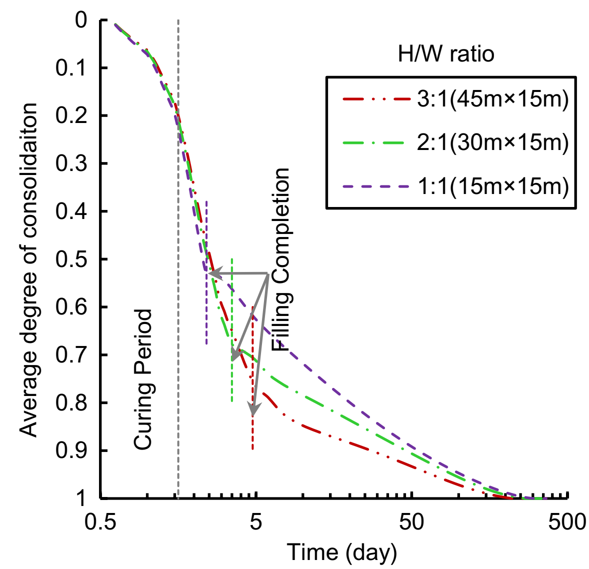

Fig. 13 Effect of H/W ratios on the consolidation process of CPB

4.2 Effect of Stope Geometry

Due to the different ore bodies and adopted stoping methods, the resultant stopes may differ in terms of size and inclination angle (Cui and Fall 2016a; Dirige et al. 2009). To investigate the effect of the stope geometry, three stopes with different height-to-width (H/W) ratios, including 1:1 (15 m × 15 m), 2:1 (30 m × 15 m) and 4:1 (45 m × 15 m) are chosen for further investigation in this study. The changes in the average degree of consolidation at a monitored point of 7 m from the stope floor with different H/W ratios are plotted in Fig. 13. It can be seen that the changes in the H/L ratio have significant impacts on the consolidation behavior of CPB, especially in the post-filling stage. Specifically, during the filling stage, the consolidation curves for the different H/L ratios follow a similar trend of change, namely, an increase in the self-weight stress with filling can significantly affect the consolidation behavior of CPB. However, after the filling takes place, there is an apparent discrepancy in the consolidation behavior of the CPB stopes with different H/L ratios, and a lower rate of consolidation is obtained in the stope with a high H/L ratio. This is because the CPB placed at a greater height exerts more overburden stress onto the monitored point. As a result, there are more volume changes in the CPB with a higher H/L

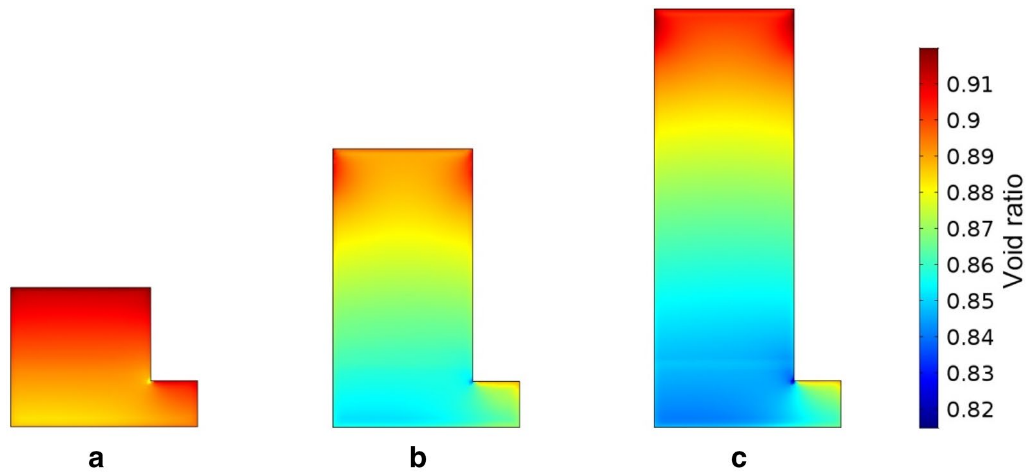

Fig. 14 Spatial distribution of void ratio of CPB with different H/W ratios after 7 days of curing: **a** 1:1 (15 m × 15 m); **b** 2:1 (30 m × 15 m); and **c** 3:1 (45 m × 15 m)

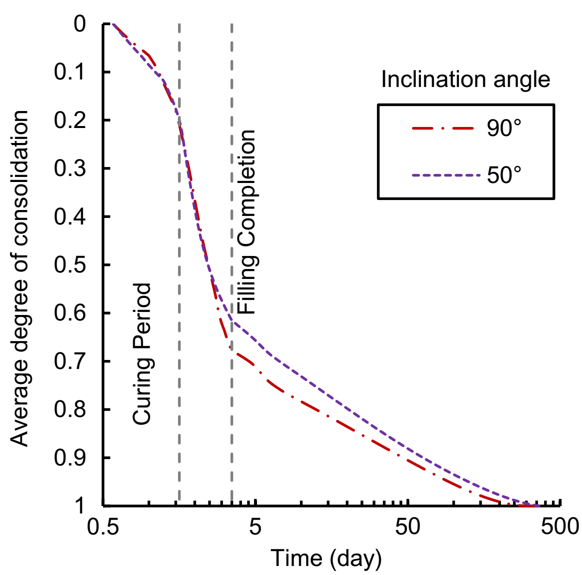

Fig. 15 Effect of inclination angles on the consolidation process of CPB

ratio (re: Fig. 14) during the filling process (void ratio decreases with higher H during the filling process due to more overburden stress), which can further increase CPB stiffness (Cui and Fall 2016a, b). Consequently, after placement, the stiffer CPB placed at a greater height can significantly reduce the rate of consolidation. Hence, CPB demonstrates distinct post-filling consolidation behavior in stopes with different H/L ratios.

Apart from the H/W ratio, the stope inclination angle is another key factor that affects the resultant backfill geometry. To investigate the effect of the stope inclination on the consolidation behavior, two dip angles of 90° and 50° are selected for further examination in this study. To isolate the effect of self-weight, the backfill height (i.e., 30 m) and backfilling strategy (i.e., filling that takes place in two stages with 1-day plug) are set to be same for these two cases. The modeling results are presented in Fig. 15, and indicate that during the curing of the plug layer and in the early onset of the second stage of filling, the development of consolidation for these two cases follows a similar trend of change. However, the differences in the degree of consolidation between these two stopes become progressively more evident after approximately 2.75 days. In particular, a lower degree of consolidation is observed in the inclined stope due to the effect of the inclination angle on the stress distribution in CPB. Previous studies on CPB (Cui and Fall 2016a, c, 2017) found that under the gravity effect, more overburden stress is transferred to the footwall (i.e., lower rock wall). As a result, non-symmetrical distribution of stress and volume changes emerge in the inclined stope, and become more pronounced with reductions in the inclination angle (see Fig. 16). Moreover, the inclined stope can further contribute to the arching effect (Cui and Fall 2016a; Suazo and Fourie 2015). As a result, vertical stress acting on the monitored point is reduced with the enhanced arching effect in the inclined stope. Therefore, there are smaller volume changes in the inclined CPB, which is clearly shown in Fig. 16 as well.

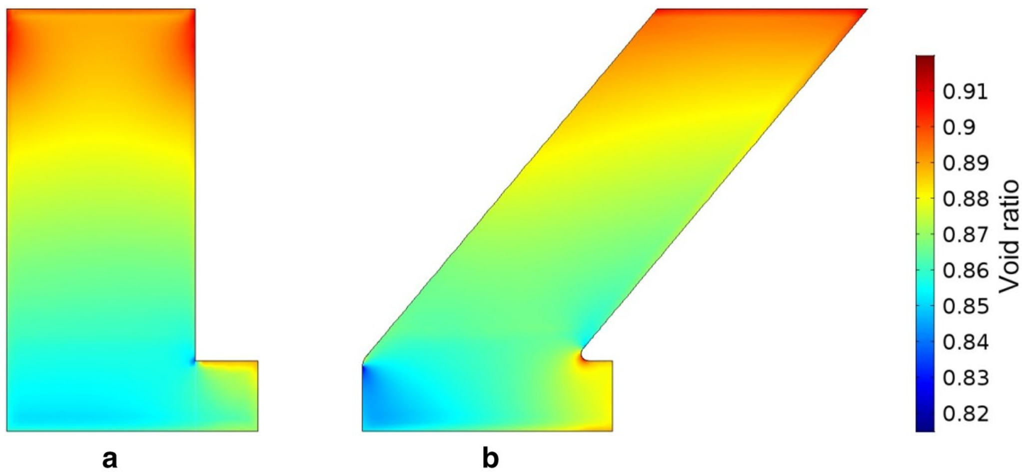

Fig. 16 Spatial distribution of void ratio of CPB with different inclination angles after 7 days of curing: **a** 90°; **b** 50°

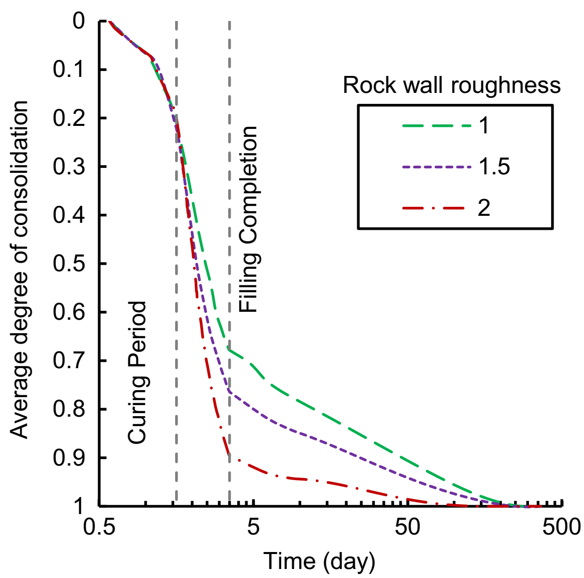

Fig. 17 Effect of rock wall roughness on the consolidation process of CPB

4.3 Effect of Rock Wall Roughness

Ore extraction operations (e.g., the use of explosives) cause the roughness of rock walls. However, the roughness of rock walls can affect the rock mass/CPB interface behavior or properties (i.e., friction angle and adhesion) and thus influence the consolidation process of CPB. To quantitatively characterize the roughness of a rock wall, the roughness index R_L (i.e., the ratio of the actual and projected lengths along the rock wall in the shearing direction) is used in this study. Three different R_L including 1 (smooth rock wall), 1.5 and 2 are selected to investigate the effect of rock wall roughness on the consolidation behavior of CPB. The modeling results are presented in Fig. 17. It is evident that the rock wall roughness has significant impacts on the consolidation behavior of the CPB. The changes in the consolidation curves which start from the second stage of filling becomes more apparent with each layer. As demonstrated in Fig. 17, with increases in the rock wall roughness, there is a greater degree of consolidation of the CPB during filling, namely, the volume changes in a stope with more rough rock walls are reduced after the completion of the stope filling process (post filling stage). This can be attributed to the increased arching effect with a CPB/rock mass interface that has more surface roughness (Cui and Fall 2017). As a result, the resultant vertical stress acting on the monitored point decreases with an increased arching effect, and thus the associated volume changes are reduced in the stope with a more rough rock wall during the post filling stage. However, it should be underlined that arching effect is only significant in narrow stopes. Several field (e.g., Thompson et al. 2009; Li et al. 2014) and modeling studies (e.g., Cui and Fall 2017) have shown that the vertical stress in narrow backfilled stope is significantly less than the overburden stress because of the arching effect, which is primarily due to the consolidation process of the CPB, and the improvement of CPB/rock-mass interface characteristics with binder hydration (Cui and Fall 2017). The consolidation of the CPB leads to the development of settlement and effective (horizontal) stresses, thus allowing shear stresses to develop at the CPB-rock interface (Fahey et al. 2009).

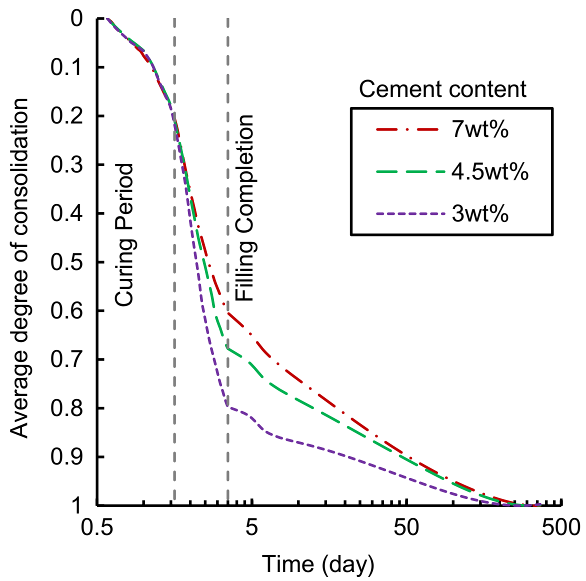

Fig. 18 Effect of cement content on the consolidation process of CPB

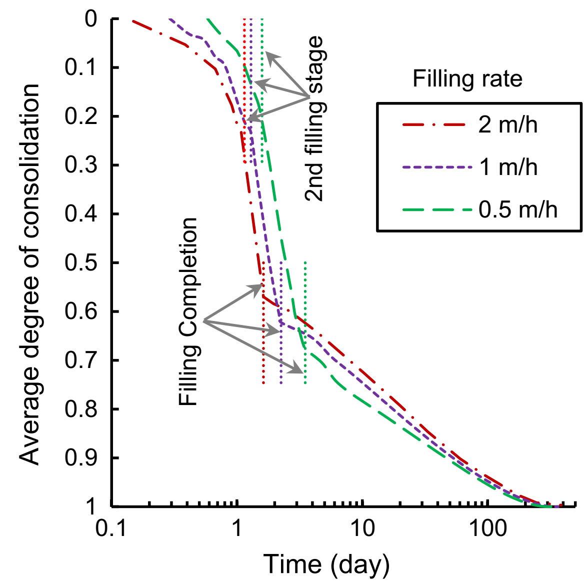

Fig. 19 Effect of filling rate on consolidation process of CPB

4.4 Effect of CPB Mix Components

The mix recipe plays a key role in the stability of CPB structures (Cui and Fall 2015a, c). In fact, cement consumption can account for up to 75% of the production costs of CPB (Fall et al. 2008; Grice 1998). In other words, a cost-effective design of CPB structures largely depends on the cement content. Due to the significance of the cement content in CPB design, three different binder contents, including 3 wt% (43.9 kg/m^3), 4.5 wt% (60.4 kg/m^3) and 7 wt% (82.2 kg/m^3) are examined to study their impacts on the consolidation behavior of CPB. The effect of cement content on the changes in the void ratio of the CPB is plotted in Fig. 18. It can be seen that the discrepancy in the consolidation behavior in CPB with different cement contents appears since the very early ages, and becomes progressively more obvious with filling and the curing that follows. Specifically, CPB with less cement content shows a higher rate of consolidation up to the completion of the filling. After completion of the filling, CPB with more cement content becomes more consolidated. This is because during the filling process, more cement content generates more cement hydration products which can further increase the stiffness of the CPB. As a result, the increase in the overburden stress by the newly placed CTB will cause a lower degree of consolidation when the cement content is higher. However, after the completion of the filling, consolidation induced by chemical shrinkage may be prevalent. As a result, CPB with a higher binder content becomes more consolidated during the post-filling stage. Therefore, this study clearly demonstrates the combined effect of hardening induced by binder hydration, overburden stress and chemical shrinkage on the consolidation behavior of CPB.

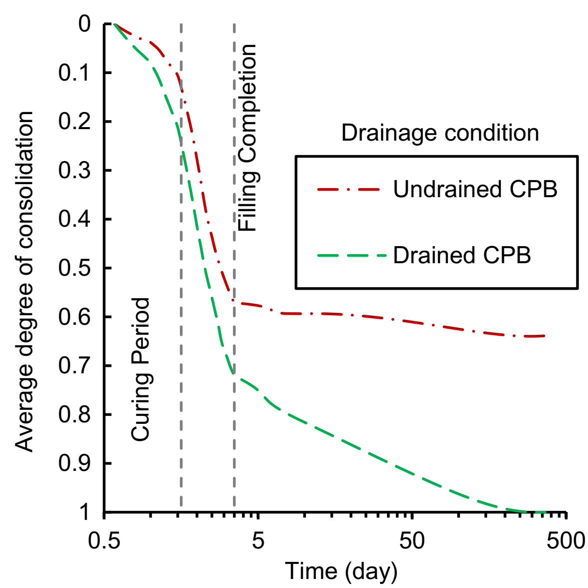

Fig. 20 Effect of drainage conditions on consolidation process of CPB

4.5 Effect of Backfilling Rate

Due to the differences in planning and scheduling underground mining, the backfilling rate may vary from one stope to another. The differences in filling rate affect the CPB operation time and thus the mining cycle and mine productivity (Khaldoun et al. 2016; Veenstra et al. 2011). Therefore, it is necessary to study the effect of the filling rate on the consolidation behavior of the CPB. In this study, a range of backfilling rates including 0.5 m/h (i.e., 12 m/day), 1 m/h (i.e., 24 m/day) and 2 m/h (i.e., 48 m/day) are simulated. The simulation results are presented in Fig. 19. It can be observed that the filling rate has a significant effect on the development of CPB consolidation. As the filling rate is reduced, there is an increase in the consolidation at the end of the filling sequence. For example, after the filling operation is carried out; i.e., 1.625 days for 2 m/h, 2.25 days for 1 m/h, and 3.5 days for 0.5 m/h, the average degree of consolidation is 0.57, 0.62 and 0.67 respectively. This is because a reduced rate of filling results in a longer filling time (and thus curing time) for a given CPB height. Consequently, the consolidation process can continue longer, and the precipitation of more hydration products can further refine the pore space. Thus, the CPB becomes more consolidated with a slower rate of filling.

4.6 Effect of Drainage Conditions

During and after pouring into underground stopes, CPB may be subjected to drained (Thompson et al. 2009, 2012) or undrained (Helinski et al. 2010; Suazo and Fourie 2015; Doherty et al. 2015) conditions. Water seepage through the barricade not only causes the dissipation of PWP, but also contributes to the consolidation of CPB. Hence, CPB placed into a stope in both drained and undrained conditions is investigated in this study. The variation in the void ratio at a monitored point is plotted in Fig. 20. For the implementation of the drainage condition, a mass flux (i.e., a product of water density and Darcy's velocity) boundary condition is applied on the barricade surface (right vertical side of the drawpoint). The obtained results demonstrate that the differences in the consolidation behavior start from the second stage of filling. As the filling operation progresses, and stops (post filling stage), the difference between the drained and undrained conditions becomes even more evident. As shown in Fig. 20, the major change in the consolidation of the CPB for the undrained condition mainly occurs during the filling stage, namely an increase in the overburden stress due to the filling operation significantly contributes to the volume changes in CPB in the undrained condition. However, the degree of consolidation in the drained condition is only 0.72 after filling is carried out, namely, greater volume changes take place in the CPB in the drained condition after filling is carried out. This is due to water drainage which can further contribute to the densification of the CPB skeleton, and is thus more favorable for the stability of the CPB structure.

The spatial distribution of the void ratio of CPB is presented in Fig. 21. It can be seen that the arching effect in the stope in the drained condition (i.e., Fig. 21b) is more obvious in comparison with that in the undrained condition (i.e., Fig. 21a). This is because more settlement occurs in the former. Correspondingly, there is also relatively more interface displacement. Therefore, a large degree of shear stress will take place on the interface resistance which can further contribute to the arching

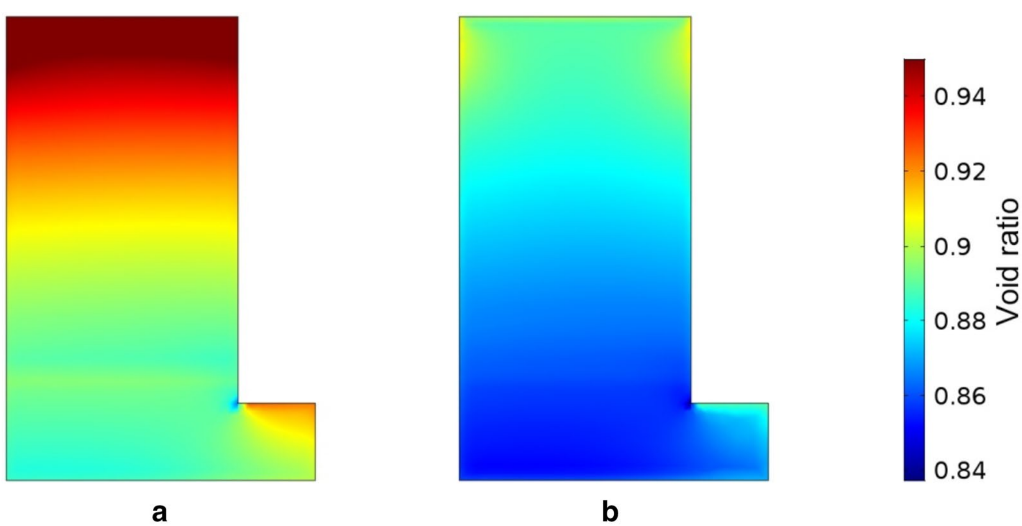

Fig. 21 Spatial distribution of void ratio of CPB under different drainage conditions after 7-days of curing: **a** undrained CPB; **b** drained CPB

effect in CPB. Moreover, it is evident in Fig. 21 that there is a pronounced change in the void ratio which occurs around the interface during the filling stages (i.e., 7 m from the stope floor) for the drained condition. This is due to the fact that there is more reduction in the pore space in the drained condition during and after plug placement. As a result, after 1-day of curing, the plug layer becomes stiffer in comparison to that in the undrained condition. Therefore, after subsequent filling, there is a greater difference in the stiffness of the CPB at the interface, which can result in strain concentration in the corresponding regime for the drained condition.

5 Conclusions

The following conclusions are made based on the obtained results in this study.

i. The in situ consolidation behavior of CPB structures is controlled by the coupled THMC processes through the effect of the self-weight of CPB, water drainage through the barricade, temperature changes induced by the heat transfer between the CPB and the surrounding environment, and chemical shrinkage caused by the development of binder hydration.
ii. The consolidation behavior of CPB structures is time-dependent, that is, the void ratio significantly varies with curing time. Moreover, changes in the void ratio mainly take place at the early ages.
iii. The rock mass conditions, including the geometry and rock wall roughness, can affect the consolidation process of CPB structures. Increased rock mass/CPB interface roughness and low inclination angles can further contribute to the development of the arching effect in CPB, which is more favorable for its stability.
iv. Cement content plays a crucial role in the consolidation process of CPB. The variations in the degree of consolidation of CPB with different cement contents are more evident from the second stage of filling, which clearly demonstrates that chemical shrinkage affects consolidation behavior.
v. A slower rate of filling can further increase the volume changes in the CPB, and thus will be beneficial for its stability. However, the differences in filling rate affect the CPB operation time and thus the mining cycles and mine productivity.
vi. Water drainage through barricades can drastically reduce the pore space of CPB, and thus contributes to the stability of retaining structures and CPB mass in stopes.

Acknowledgements
Not applicable.

Authors' contributions
LC and MF authors significantly contributed to the research presented in this manuscript and its writing. Both authors read and approved the final manuscript.

Funding
The authors thank the Natural Sciences and Engineering Research Council of Canada (NSERC) and the University of Ottawa for their financial support.

Availability of data and materials
The data used and/or assessed during this research are included in the present manuscript.

Competing interests
The authors declare that they have no competing interests.

Received: 18 November 2019 Accepted: 31 January 2020
Published online: 27 April 2020

References

Ai, Z. Y., & Hu, Y. D. (2015). Multi-dimensional consolidation of layered poroelastic materials with anisotropic permeability and compressible fluid and solid constituents. *Acta Geotechnica, 10*(2), 263–273. https://doi.org/10.1007/s11440-013-0296-6.
Belem, T., Harvey, A., Simon, R., Aubertin, M. (2004). Measurement and prediction of internal stresses in an underground opening during its filling with cemented fill. In: Proceedings of 5th international symposium on ground support in mining and underground construction, Perth, Australia, pp 28–30.
Benzaazoua, M., Fall, M., & Belem, T. (2004). A contribution to understanding the hardening process of cemented. *Minerals Engineering, 17*(2), 141–152. https://doi.org/10.1016/j.mineng.2003.10.022.
Biot, M. A. (1955). Theory of elasticity and consolidation for a porous anisotropic solid. *Journal of Applied Physics, 26*(2), 182–185. https://doi.org/10.1063/1.1721956.
Ceccato, F., & Simonini, P. (2016). Numerical study of partially drained penetration and pore pressure dissipation in piezocone test. *Acta Geotechnica*. https://doi.org/10.1007/s11440-013-0285-9.
Comsol (2015) Comsol Multiphysics 5.1. http://www.comsol.com.
Cui, L., & Fall, M. (2015a). A coupled thermo-hydro-mechano-chemical model for cemented tailings backfill. *InInternational EAGE Workshop on Geomechanics and Energy, 50*, 396–414. https://doi.org/10.1016/j.tust.2015.08.014.
Cui, L., Fall, M. (2015b). Modeling and simulation of the consolidation behaviour of cemented paste backfill. In: Proceedings of 2015 Comsol conference, Boston, MA, USA, pp 1–5.
Cui, L., Fall, M. (2015c) Multiphysics modelling of the behaviour of cemented tailings backfill materials. In: Proceedings of international conference on civil, structural and transportation engineering, Ottawa, ON, Canada, pp (330)1–7.
Cui, L., & Fall, M. (2016a). Multiphysics model for consolidation behaviour of cemented paste backfill. *International Journal of Geomechanics, 040160771*, 0401607723. https://doi.org/10.1061/(asce)gm.1943-5622.0000743.
Cui, L., & Fall, M. (2016b). An evolutive elasto-plastic model for cemented paste backfill. *Computers and Geotechnics, 71*, 19–29.
Cui, L., & Fall, M. (2016c). Mechanical and thermal properties of cemented tailings materials at early ages: Influence of initial temperature, curing stress and drainage conditions. *Construction and Building Materials, 125*, 553–563. https://doi.org/10.1016/j.conbuildmat.2016.08.080.
Cui, L., & Fall, M. (2017). Multiphysics modeling of arching effects in fill mass. *Computers and Geotechnics, 83*, 114–131. https://doi.org/10.1016/j.compgeo.2016.10.021.
Dirige, A., McNearny, R., Thompson, D. (2009). The effect of stope inclination and wall rock roughness on back-fill free face stability. In: Proceedings of

the 3rd Canada–US rock mechanics symposium, Toronto, ON, Canada, pp (4152)1–12.
Doherty, J. P., Hasan, A., Suazo, G. H., & Fourie, A. (2015). Investigation of some controllable factors that impact the stress state in cemented paste backfill. *Canadian Geotechnical Journal, 52*(12), 1901–1912. https://doi.org/10.1139/cgj-2014-0321.
El Mkadmi, N., Aubertin, M., & Li, L. (2013). Effect of drainage and sequential filling on the behavior of backfill in mine stopes. *Canadian Geotechnical Journal, 51*(1), 1–15. https://doi.org/10.1139/cgj-2012-0462.
Fahey, M., Helinski, M., & Fourie, A. (2009). Some aspects of the mechanics of arching in backfilled stopes. *Canadian Geotechnical Journal, 46*(11), 1322–1336. https://doi.org/10.1139/T09-063.
Fall, M., Belem, T., Samb, S., & Benzaazoua, M. (2007). Experimental characterization of the stress–strain behaviour of cemented paste backfill in compression. *Journal of Materials Science, 42*(11), 3914–3922. https://doi.org/10.1007/s10853-006-0403-2.
Fall, M., Benzaazoua, M., & Saa, E. (2008). Mix proportioning of underground cemented tailings backfill. *Tunnelling and Underground Space Technology, 23*(1), 80–90. https://doi.org/10.1016/j.tust.2006.08.005.
Fall, M., Célestin, J., & Sen, H. (2010). Potential use of densified polymer-pastefill mixture as waste containment barrier materials. *Waste Management, 30*(12), 2570–2578. https://doi.org/10.1016/j.wasman.2010.07.016.
Fall, M., Nasir, O., Cui, L., Han, F. (2015). Coupled modeling of the strength development and distribution within cemented paste backfill structure. In: Proceedings of 49th US rock mechanics/geomechanics symposium, pp 587–595.
Fang, K., & Fall, M. (2018). Effects of curing temperature on shear behaviour of cemented paste backfill-rock interface. *International Journal of Rock Mechanics and Mining Sciences, 112,* 184–192.
Ghirian, A., Fall, M. (2013). experimental investigations of the thermo-hydro-mechanical-chemical behavior of cemented paste backfill. In: Proceedings of 23rd world mining congr, Montreal, Canada, pp (378)371–311.
Ghirian, A., & Fall, M. (2014). Coupled thermo-hydro-mechanical-chemical behaviour of cemented paste backfill in column experiments: Part II: Mechanical, chemical and microstructural processes and characteristics. *Engineering Geology, 170,* 11–23. https://doi.org/10.1016/j.enggeo.2013.12.004.
Ghirian, A., & Fall, M. (2015). Coupled behavior of cemented paste backfill at early ages. *Geotechnical and Geological Engineering, 33*(5), 1141–1166. https://doi.org/10.1007/s10706-015-9892-6.
Grice, T. (1998) Underground mining with backfill. In: Proceedings of the 2nd annual summit-mine tailings disposal systems, Australian, pp 234–239.
Haiqiang, J., Fall, M., & Cui, L. (2016). Yield stress of cemented paste backfill in sub-zero environments: Experimental results. *Minerals Engineering, 92,* 141–150. https://doi.org/10.1016/j.mineng.2016.03.014.
Han, F., Zhang, Z., Liu, J., & Yan, P. (2016). Hydration kinetics of composite binder containing fly ash at different temperatures. *Journal of Thermal Analysis and Calorimetry, 124*(3), 1691–1703. https://doi.org/10.1007/s10973-016-5295-z.
Hassani, F., Ouellet, J., Servant, S. (2001). In situ measurements in a paste backfill: Backfill and rock mass response in the context of rockburst. In: Proceedings of 17th international mining congress and exhibition of Turkey, Ankara, Turkey, pp 165–175.
Helinski, M., Fahey, M., & Fourie, A. (2010). Behavior of cemented paste backfill in two mine stopes: Measurements and modeling. *Journal of Geotechnical and Geoenvironmental Engineering, 137*(2), 171–182. https://doi.org/10.1061/(ASCE)GT.1943-5606.0000418.
Jehring, M. M., & Bareither, C. A. (2016). Tailings composition effects on shear strength behavior of co-mixed mine waste rock and tailings. *Acta Geotechnica, 11*(5), 1147–1166. https://doi.org/10.1007/s11440-015-0429-1.
Khaldoun, A., Ouadif, L., Baba, K., & Bahi, L. (2016). Valorization of mining waste and tailings through paste backfilling solution, Imiter operation, Morocco. *International Journal of Mining Science and Technology, 26*(3), 511–516. https://doi.org/10.1016/j.ijmst.2016.02.021.
Li, L., & Aubertin, M. (2009). Numerical investigation of the stress state in inclined backfilled stopes. *International Journal of Geomechanics, 9*(2), 52–62. https://doi.org/10.1061/(ASCE)1532-3641(2009)9:2(52).
Li, L., Aubertin, J. D., & Dubé, J.-S. (2014). Stress distribution in a cohesionless backfill poured in a silo. *The Open Civil Engineering Journal, 8,* 1–8. https://doi.org/10.2174/1874149501408010001.
Potvin, Y., & Thomas, E. (2005). *Handbook on mine fill*. Crawley, WA, Australia: Australian Centre for Geomechanics.
Schindler, A. K., Folliard, K. J. (2003). Influence of supplementary cementing materials on the heat of hydration of concrete. In: Proceedings of advances in cement and concrete IX conference, Colorado, pp 17–26.
Shahsavari, M., Grabinsky, M. (2015). Mine backfill pore water pressure dissipation: Numerical predictions and field measurements. In: Proceedings of GeoQuébec, Québec city, Canada, pp 1–8.
Suazo, G., Fourie, A. (2015). Numerical simulation of blast response of cemented paste backfills. In: Proceedings of the 15th Pan-American conference on soil mechanics and geotechnical engineering, Buenos Aires, Argentina, pp 2394–2401.
Tariq A (2012) Synergistic and environmental benefits of using cement kiln dust with slag and fly ash in cemented paste tailings. Ph.D. Thesis, University of Western Ontario.
Terzaghi, K. (1943). *Theory of consolidation*. Hoboken, NJ, USA: John Wiley & Sons Inc.
Thompson, B., Bawden, W., & Grabinsky, M. (2012). In situ measurements of cemented paste backfill at the Cayeli Mine. *Canadian Geotechnical Journal, 49*(7), 755–772. https://doi.org/10.1139/t2012-040.
Thompson, B., Grabinsky, M., Bawden, W., Counter, D. (2009). In-situ measurements of cemented paste backfill in long-hole stopes. In: Proceedings of the 3rd CANUS rock mechanics symposium, Toronto, pp 197–198.
Veenstra, R., Bawden, W., Grabinsky, M., Thompson, B. (2011). An approach to stope scale numerical modelling of early age cemented paste backfill. In: Proceedings of 45th US rock mechanics/geomechanics symposium, San Fransisco, California, USA, pp (274)1–7.
Williams, T. J., Denton, D. K., Larson, M. K., Rains, R. L., Seymour, J. B., Tesarik, D. R. (2001). Geomechanics of reinforced cemented backfill in an underground stope at the Lucky Friday Mine. Report 9655, National Institute for Occupational Safety and Health, Pittsburgh, PA.
Yilmaz, E. (2018). Stope depth effect on field behaviour and performance of cemented paste backfills. *International Journal of Mining, Reclamation and Environment, 32*(4), 273–296.
Yilmaz, E., Kesimal, A., & Ercikdi, B. (2003). The factors affecting the strength and stability of paste backfill. *Yerbilimleri–Turkish Earth Sciences, 28*(2), 155–169.
Zhang, Q., Zhang, J., Guo, S., Gao, R., & Li, W. (2015). Design and application of solid, dense backfill advanced mining technology with two pre-driving entries. *International Journal of Mining Science and Technology, 25*(1), 127–132. https://doi.org/10.1016/j.ijmst.2014.12.008.

Publisher's Note